

Press, London, 1959), p. 397.

⁴⁷V. H. Dibeler, R. M. Reese, *J. Chem. Phys.* **31**, 282 (1959).

⁴⁸J. D. Morrison, *J. Chem. Phys.* **21**, 1767 (1953).

⁴⁹D. A. Hutchison, *Atomic Collision Processes*, (North-Holland Publishing Company Amsterdam, 1964) p. 443.

⁵⁰R. K. Curran, *J. Chem. Phys.* **38**, 2974 (1963).

⁵¹I. O. Allison, R. D. Sedgwick, in "Proceedings of the International Mass Spectrometry Conference," Berlin, 1967, p. 20 (to be published).

⁵²V. S. Troitskii, *Zh. Eksperim. i Teor. Fiz.* **41**, 389 (1961) [English transl.: *Sov. Phys. - JETP* **14**, 281 (1962)].

e-H Resonances in the 2*p* Excitation Channel*

J. William McGowan, J. F. Williams,[†] and E. K. Curley

Gulf General Atomic Incorporated, San Diego, California 92112

(Received 23 December 1968)

The cross section for the electron-impact excitation of the hydrogen atom to the 2*p* radiative state has been measured from the threshold (at 10.2 eV) to 50 eV. Primary interest is given to the region between the threshold and the *n*=4 level of the hydrogen atom, where several resonances have been identified. An electron-beam resolution of 0.07 eV has been used to study the resonances, while a resolution of 0.18 eV has been used to determine the general behavior of the cross section. Below *n*=3 the ¹S resonances appear to agree with the theoretical predictions, but in the case of the higher angular-momentum ¹D resonance, the agreement between present theory and experiment is poor. Balmer- α excitation is discussed.

I. INTRODUCTION

Theoretical and experimental investigations of the electron-impact excitation of the ground-state hydrogen atom to its first radiative state, the 2*p* state, recently have been reviewed.¹ For electron energies greater than 200 eV, the measured energy dependence of the experimental cross section is best predicted by the Born approximation to the total wave equation, while above about 60 eV, the three-state 1*s*-2*s*-2*p* close-coupling approximation calculations seem to fit the experimental results. There is no calculation which agrees with the experimental values from about 60 eV down to the vicinity of the threshold.

Within several volts of the threshold the three-state close coupling approximation¹⁻⁶ again predicts cross-section values approaching to within 40% the values observed experimentally.⁷⁻⁹ The effect of including higher states in the approximation, i. e., bringing the 3*s*, 3*p*, and 3*d* states into the 1*s*-2*s*-2*p* coupling, is generally to lower the predicted values by about 20%. The effect of adding to the 1*s*-2*s*-2*p* approximation some 20 potential-energy terms which describe electron-

electron correlation¹⁰ is to generally reduce the predicted values by another 10%. However, as discussed in this paper, over the first few electron volts above the threshold, such predicted values are still higher than measured values by about 10%. These discrepancies may well be accounted for by including the full effect of the polarization of the excited states of the target atom.¹¹

In the close-coupling approximation, it has been shown, for the *n*=2 and *n*=3 levels, that including coupling to states of the given level results in resonance structure predictions both above and below that level. Recent experimental work^{9,12} has confirmed the existence of such resonances in the 2*p* channel just above the *n*=2 threshold.

Recent calculations¹³ of the ¹D elastic-scattering resonance below *n*=2 show that for this *l*=2 or *D* state (and perhaps all angular-momentum states *l*≥2), the position of the resonance as calculated within the close-coupling approximation depends critically upon the inclusion of higher-lying states of the target atom.

In this paper, attention is given to the 2*p* excitation threshold and the resonance above the *n*=2

level as well as to those below and above the $n=3$ level and cascade from the $3s$ and $3d$ levels to the $2p$ state of the atom.

II. INSTRUMENTATION AND EXPERIMENTAL APPROACH

The basic apparatus as it pertains to the production of monoenergetic electrons and the H-atom beam is essentially unchanged from that described previously.¹⁴ The pertinent features are shown in Figs. 1 and 2.

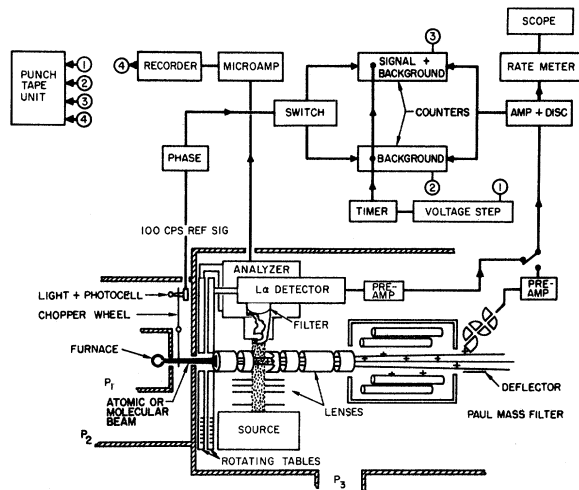


FIG. 1. Diagram of the three-chamber beam machine and the main electronic equipment used in collecting and recording the experimental data.

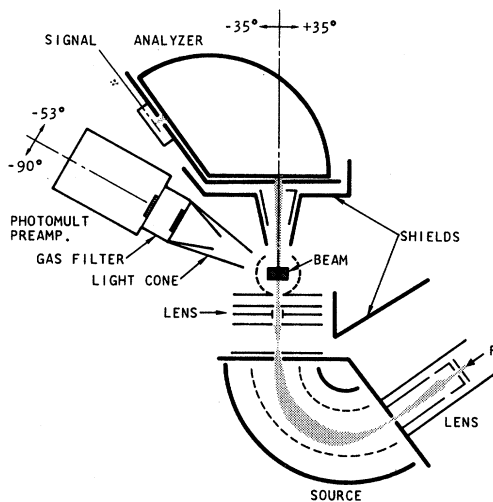


FIG. 2. Schematic diagram showing the collision region, the photomultiplier, and the source and analyzing 127° electrostatic electron energy selectors. The analyzer can be rotated from $+35^\circ$ to -35° , while the photomultiplier can be rotated from -90° to -53° .

A beam containing more than 85% hydrogen atoms is produced in a tungsten furnace which is heated to approximately 2700°K . The furnace is contained in the first of three separately pumped vacuum chambers, the source, buffer, and interaction chambers, in which the pressures are approximately 10^{-4} , 10^{-6} , and 10^{-7} Torr, respectively, when the beam is flowing. The pressure buffer chamber also contains the atom beam modulator, which is a rotating tooth chopper wheel, the teeth of which intercept the hydrogen atom beam 100 times per second.

An electron beam with an energy resolution near 0.07 eV is produced in a 127° electrostatic electron energy selector, the details of which are shown in Fig. 2. A second, identical selector is used as an analyzer. It is mounted on a disc, which in this experiment can be rotated through an angle of $\pm 35^\circ$ with respect to the electron beam. Immediately before the input slit of the analyzer is a crossed electric field collector which is used to monitor the electron current during the course of the experiment. When the electric field is removed, the electron beam passes through this collector region and into the analyzer, where the mean beam energy and energy spread are determined. The residual magnetic field over the interaction region and over the total electron-beam path length is less than 20 mG.

Mounted on a separate rotatable table in an Electro-Mechanical Research Incorporated photomultiplier, which has 18 silver-magnesium dynodes, a side window made of lithium fluoride, and a potassium bromide photocathode. The spectral response of the tube peaks at 1200 \AA and drops 2 dB at 1050 and 1500 \AA . The active cathode diameter is 1 cm^2 . Immediately in front of the photomultiplier is an oxygen cell through which dry oxygen continuously flows. The effective absorption thickness of the oxygen gas is 1-cm length times an atmosphere pressure. The absorption properties of oxygen¹⁵ are such that it is opaque to radiation in this wavelength range except at seven windows, one of which occurs at 1216 \AA Lyman α . Thus the oxygen filter strongly attenuates ultraviolet radiation excited by electron collision with residual gas in the vacuum chamber and residual H_2 in the atomic hydrogen beam. Also, all countable bremsstrahlung radiation is eliminated in this experiment.

The photomultiplier looks through the filter directly into the interaction region. Care was taken to ensure that the photomultiplier did not have a line of sight to any surface upon which the electron beam impacted. In this experiment, the Lyman- α radiation, i. e., electric-dipole radiation coming from the decay of the $2p$ excited state of atomic hydrogen, has been detected.

Consequently, the angular distribution of the radiation intensity per unit solid angle in the direction θ , i. e., $I(\theta)$, can be expressed¹⁶ as

$$I(\theta) = [I_0(1 - P \cos^2\theta)] / [4\pi(1 - P/3)] ,$$

where P is the constant referred to as the polarization of the radiation which is constant for a given electron energy, θ is the angle between the direction of photon emission and the direction of incident electron beam, and I_0 is the total intensity. For observations at 54.5° and 125.5° , $\cos^2\theta = \frac{1}{3}$ and therefore $I(\theta)$ is independent of the polarization. Consequently, the signal measured at these angles is directly proportional to the total cross section.

The major problem in our experiment arose from the collection of data over an extended period of time. In the excitation threshold region where the number of photons emitted tends to be small, when one takes into account the density of the hydrogen atom beam, approximately 10^9 particles/cm³, the current of the electrons, approximately 5×10^{-8} A, the solid angle of observation, approximately 10^{-2} sr, and the absorption in the oxygen filter and in the windows of the counter, the number of photons available for counting is about 10 per min. Therefore, it is necessary to collect data over an extended period of time in order to obtain statistically meaningful results. In order to minimize the errors which could arise from long-time fluctuations and noise considerations, the total excitation spectrum as a function of electron energy was obtained by making many rapid scans over a given electron energy interval and summing those many scans together.

The excitation function is broken into a number of equal intervals, a number normally taken between 40 and 100. The energy increment could be varied between 0.01 and 0.10 eV, with 0.10 eV being used with high current, lower resolution runs. The instrument is programmable. At each energy, we normally reside 1 min. Once one run of the spectrum is completed, the system begins again. In our experiments, the following information is recorded: the energy of the electrons, the current of the bombarding electrons, the number of signal counts plus background, and the number of counts associated with background alone. The difference between the latter two numbers gives the signal associated with electron-hydrogen atom excitation. This information is digitally recorded on punched tape, which at the completion of an experiment is processed by computer. Such processes as error analysis, data smoothing, curve fitting, etc., are facilitated by the computer.

At the same time as the above information is recorded, it is desirable to know that the density of hydrogen atoms is kept constant. In this ex-

periment, both the pressure in the furnace chamber and the temperature of the furnace are monitored as a function of time. To given an estimate of the temperature of the furnace, a photodiode looks along the beam axis through the mechanical chopper at the furnace. The modulated signal output from this diode is directly related to the temperature of the furnace.

While our primary interest has been in the threshold excitation energy regions, we have looked at electron-hydrogen atom collisions up to an electron energy in excess of 200 eV. These high energy measurements were used to normalize our results independently to the Born approximation at high energies. This will be discussed in detail in the next section.

Just as important as the determination of the absolute excitation cross section is the absolute measurement of the electron energy scale. Since it is difficult to obtain an instrumental determination of this scale, it is preferable to calibrate the scale by referring it to some known process. Both the $2p$ excitation threshold (since it is finite at threshold) and the ionization threshold have been used to locate the absolute electron energy scale. Both measurements are constant to within ± 0.015 eV over a 4-day period provided the ionization threshold is a nonlinear function of the excess energy as previously suggested.¹⁴ An ionization efficiency curve in the vicinity of the ionization threshold is taken (a) before and after each run, and (b) every 10 to 12 h during a 90-h run.

III. RESULTS AND DISCUSSION

Determination of Absolute Cross Section

Previous experiments⁷ have demonstrated that, for electron energies above 200 eV, the shape of the $1s$ - $2p$ excitation cross section is similar to the shape predicted by the Born approximation, which may then serve as a basis for normalization of data at energies above about 200 eV. In the present experiment, the apparatus was not designed to operate at electron energies much in excess of 150 eV. The experimental values extend up to 210 eV, which permits only a limited accuracy to be obtained in the normalization procedure because of the small overlap through the energy interval where the Born approximation is thought to hold. When our data are independently normalized to the Born approximation, they agree with published data^{7, 8} well within the ascribed $\pm 10\%$ error.

In order to obtain a larger energy region over which to normalize the present data, we referenced our data to the data of Long, Cox, and Smith,⁸ who normalized their data to the value $0.486\pi a_0^2$, which was obtained from the Born ap-

proximation at 200 eV with corrections made for cascading. Their estimated accuracy is $\pm 2\%$. In order to make a comparison with their data, it was necessary to correct their data for the polarization of the emitted light. To do this, we have used the recent measurements of Lyman- α polarization which have been reported by Fite *et al.*¹⁷ Because our primary interest has been in the details of excitation and resonance formation within the energy region 10 to 13 eV, it appears sufficient to obtain an absolute cross-section scale in the above manner, particularly when the agreement between the two sets of data is so good. Figure 3 shows the present data and those of Long, Cox, and Smith. Although the relative uncertainty of the present data is $\pm 5\%$ (greater than one standard deviation), the agreement between the two sets of data is within a few percent, which, in turn, lends support to the accuracy of the polarization data.¹⁷

It is significant that the measured cross section below 60 eV and even in the vicinity of threshold continues to lie below the best theoretical prediction. As can be seen in Fig. 4, the measurements in the threshold region lie between 20% and 30% below the three-state close-coupling calculation. Until quite recently, a dilemma existed in the case of 2s excitation, where it appeared that the theoretical calculations were a factor of 2 larger than the experimental values. However, new measurements by Fite *et al.*,¹⁸ have shown that the earlier measurements of 2s excitation were insufficient in that no correction was made for the polarization of the radiation from the electrostatically quenched state. Now that this correction has been made, the experimental values lie approximately the same interval below the calculations as do the 2p data. Even though the large discrepancy between the 2s and 2p excitation data

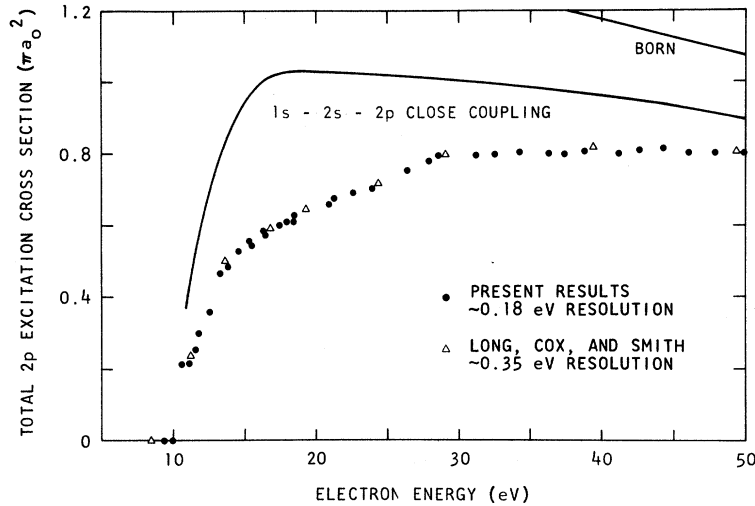


FIG. 3. Total 2p excitation cross section shown as a function of incident electron energy from threshold to 50 eV. The present data (●) obtained with an electron energy resolution of 0.18 eV are shown normalized at 200 eV to those of Long, Cox, and Smith, who used an electron-beam energy resolution of 0.35 eV.

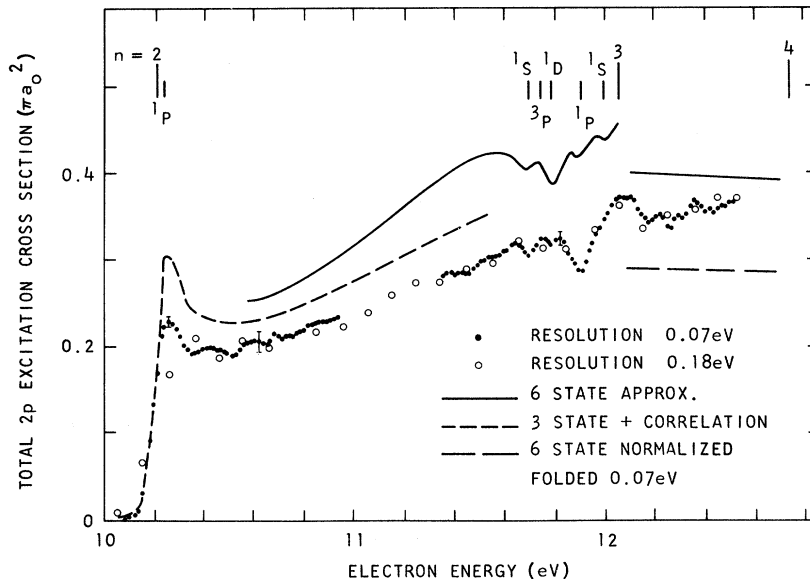


FIG. 4. Total 2p excitation cross section as a function of incident electron energy from threshold to 12.6 eV. Experimental data, obtained using both high (0.07 eV) and low (0.18 eV) resolution of the incident electron-beam energy, are compared with the six-state close-coupling predictions and the "three-state close coupling plus electron correlation" predictions into which has been folded our electron energy spread of 0.07 eV.

is no longer present, one is still perplexed by the fact that the experimental values continue to lie below the theoretical values. Perhaps, as has been suggested by Burke *et al.*, part of the problem is associated with the normalization of the data to the Born approximation at large energies and part may be associated with the inadequacy of the Born approximation at these energies. Certainly these suggestions must be tested by an independent measurement of the absolute cross section.

Resonances Above $n = 2$

Our measurements of the "shape" resonances immediately above the $n = 2$ level have been reported recently.⁹ It was shown (see Fig. 4) that our experimental results through the first resonance peak agree exceptionally well with the theoretical prediction (refer to Table I). However, these measurements suggest that perhaps this peak is broader than is suggested by the theory, which takes into account, through close coupling, the three lowest states plus the interaction between the electrons.

An interesting find was that immediately above this first peak is a small statistically real second peak which at the time of the experiments was not defined by theory. Since then, through a three-state close-coupling calculation, Marriott and Rotenberg¹⁹ have shown that similar structure also appears in the 1P channel and is likely to be the interference portion of the first resonance.

TABLE I. Structure in $2p$ excitation curve.

Energy (eV)	Description of structure	Comments
10.20 ± 0.02	Steep slope	Onset
10.29 ± 0.02	First max	Predicted 1P "shape" resonance
10.45 ± 0.03	Second max	Statistically real
10.65 ± 0.03	Third max	Not statistically real
11.65 ± 0.03	Small min	Predicted 1S resonance
11.77 ± 0.02	Possible min	Predicted 1D and 3P resonances, may be 3P resonance
11.89 ± 0.02	Large min	Predicted 1P resonance, dominantly 1D resonance
12.06 ± 0.04	Broad max	"Shape" resonance at $n=3$ threshold
12.16 ± 0.05	Min	
12.23 ± 0.05	Small max	
12.35 ± 0.05	Small max	

The alternate suggestions, of course, are that this is the second of a series of "shape" resonances which appear just above the inelastic threshold or that the structure appears in another channel or that this structure is part of the oscillatory structure calculated by Damburg and Gailitis³ and by Omidvar.²⁰ The third ill-defined structure has not as yet been associated with any particular inelastic channel.

In order to make certain that the second peak was statistically real, it was necessary to collect data for an average of 2 h per point over a total period in excess of 120 h.

Resonances Below $n = 3$

The data in the vicinity of $n = 2$ and those in the vicinity of $n = 3$ have been normalized to lower resolution data (the open circles in Fig. 4), which in turn have been fixed to the data of Long *et al.*⁸ In the high resolution data just below $n = 3$, resonance structure is clearly defined. At first glance it is quite similar to that resulting from the six-state close-coupling approximation calculation¹⁰ with the electron energy distribution folded in. However, there is in the calculation a large shoulder to the left of the resonances which does not appear in the experimental data. Furthermore, the position of the major theoretical valley does not correspond to the position of the major experimental valley; in fact, it appears to be shifted down nearly 0.1 eV.

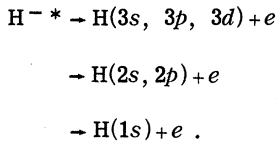
In both the experimental and theoretical results the lowest 1S resonance agrees in position and in width. With the energy distribution folded into the theoretical curve, the 3P resonance is not clearly defined. The large 1D resonance which appears in the theory near 11.8 eV does not appear in the experimental results. However, the dominant feature in the experimental curve agrees well in position but not width with the lowest 1P resonance. It is our contention, to be discussed below, that this structure is indeed the 1D resonance. In some experimental curves the second 1S resonance is recognizable along the face of the sharp rise of the large resonance. The positions of the dominant features of the experimental curve along with the dominant features in the theoretical curve are given in Table I.

It has recently been demonstrated¹³ that just below the inelastic threshold the first 1D resonance observed in the elastic-scattering channel²¹ is not described well by the $1s-2s-2p$ close-coupling calculations. However, this approximation does describe the position and width of the lowest 1S and 3P resonance with reasonable accuracy. When the $3s$, $3p$, and $3d$ states were included in the calculation, the position of the calculated 1D resonance markedly shifted to be in much better agreement with experiment, suggesting that the

inclusion of only the lower states does not carry in sufficient information about the higher angular-momentum states. No doubt, the situation is similar in the $2p$ channel where six states do not appear to be sufficient to describe the lowest 1D resonance. The addition of more states, different states, electron-electron correlation, or perhaps polarization of the excited states appears to be needed to fit the calculated 1D resonance with the experimental results.

Resonance Structure Above $n = 3$

The large peak in the vicinity of $n = 3$ is most likely due to a "shape" resonance just above the onset of $n = 3$. This resonance is free to decay in three ways:



Lyman- α production will be observed through two of these: through cascade from either the $3s$ or $3d$ state to the $2p$ level which subsequently decays, or from direct decay of the $2p$ level. It has been pointed out by Burke *et al.*, that the compound state above $n = 2$ decays dominantly to the $n = 2$ level. One can imagine that, in a similar way, the compound state above $n = 3$ will predominantly decay to the $n = 3$ states to be reflected in the Lyman- α primarily through cascade. The position of this resonance and subsequent structure has been recorded in Table I. From a careful examination of the lower resolution data, we have been able to determine that resonance structure also appears in the vicinity of $n = 4$ and higher.

Excitation of Balmer α

No direct measurements of the Balmer- α excitation have been made; however, that portion of the Lyman- α production cross section above $n = 3$ and below $n = 4$ contains information from cascade of the $3s$ and $3d$ states to the $2p$ state. Although we know the direct $2p$ excitation calculations to be wrong in magnitude below and above $n = 3$, the relative error is not likely to change greatly through this region. Therefore by normalizing the calculations to the data below $n = 3$, we obtain an estimate of direct excitation above $n = 3$. The result of the normalization is labeled "6-state normalized" in Fig. 4. The difference between this line and the data then gives some idea of cascade. Since this is a small difference between large numbers, the uncertainty is large. This is represented by the large band shown in Fig. 5.

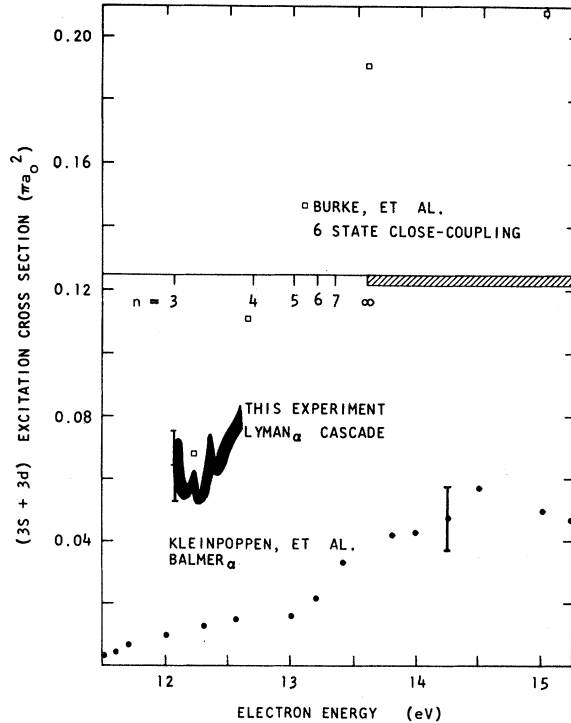


FIG. 5. Estimated $(3s+3d)$ excitation cross section shown as a function of incident-electron energy. The width of the broad line reflects the uncertainty in the theoretical to experimental normalization.

These numbers can now be directly compared with the experimental measurements of Kleinpoppen and Kraiss²² and calculations by Burke, Ormonde, and Whitaker.⁴ This comparison is shown in Fig. 4. Our data lie above the experimental points but below the theoretical values. The interval by which our data lies below theory is consistent with other comparisons of theory and experiment; however, the inconsistency between our numbers and the direct measurement is not completely understood.

IV. SUMMARY

There is qualitative agreement between the close-coupling calculations and the present experiments. The predicted resonances above $n = 2$ and below $n = 3$ have been observed; however, the predicted position of the 1D resonance does not appear to agree with the experimental position, probably because not enough information concerning the higher angular-momentum states is carried into the calculation by the lowest six states used in the close-coupling calculation. In contrast to that comparison, the six-state approximation does appear to describe the 1S resonances well.

Through the first few electron volts of energy above the $2p$ excitation threshold, the measured cross section, which is normalized to the Born approximation at energies in excess of 200 eV,

lies below the best theoretical calculation. Similarly, an estimate of the Balmer- α excitation cross section lies below the predicted values but above the only directly measured value.

*Research sponsored by NASA Goddard Space Flight Center under Contract NAS5-11150, and Gulf General Atomic private funds.

†Gulf General Atomic Associate Scientist.

¹B. L. Moiseiwitsch and S. J. Smith, *Rev. Mod. Phys.* 40, 238 (1968).

²P. G. Burke, *Proc. Phys. Soc. (London)* 82, 443 (1963).

³R. J. Damburg and M. K. Gailitis, *Proc. Phys. Soc. (London)* 82, 1068 (1963).

⁴P. G. Burke, S. Ormonde, and W. Whitaker, *Proc. Phys. Soc. (London)* 92, 319 (1967).

⁵J. Macek and P. G. Burke, *Proc. Phys. Soc. (London)* 92, 351 (1967).

⁶P. G. Burke and A. J. Taylor, *Proc. Phys. Soc. (London)* 88, 549 (1966).

⁷W. L. Fite and R. T. Brackmann, *Phys. Rev.* 113, 1151 (1956); W. L. Fite, R. F. Stebbings, and R. T. Brackmann, *ibid.* 116, 356 (1959).

⁸R. L. Long, D. M. Cox, and S. J. Smith, *J. Res. Natl. Bur. Std.* 72A, 521, (1968).

⁹J. F. Williams and J. Wm. McGowan, *Phys. Rev. Letters* 21, 719 (1968).

¹⁰A. J. Taylor and P. G. Burke, *Proc. Phys. Soc.*

(London) 92, 336 (1967).

¹¹R. J. Damburg and S. Geltman, *Phys. Rev. Letters* 20, 485 (1968).

¹²G. E. Chamberlain, S. J. Smith, and D. W. O. Heddle, *Phys. Rev. Letters* 12, 647 (1964).

¹³S. J. Ormonde, J. McEwen, and J. Wm. McGowan, to be published.

¹⁴J. Wm. McGowan and E. M. Clarke, *Phys. Rev.* 167, 43 (1968).

¹⁵K. Watanabe, E. C. Y. Inn, and M. Zelikoff, *J. Chem. Phys.* 21, 1021 (1953).

¹⁶I. C. Percival and M. J. Seaton, *Phil. Trans. Roy. Soc. (London)* 251, 113 (1958).

¹⁷W. R. Ott, W. E. Kauppila, and W. L. Fite, *Phys. Rev. Letters* 19, 1361 (1967).

¹⁸W. L. Fite, W. E. Kauppila, and W. R. Ott, *Phys. Rev. Letters* 20, 409 (1968).

¹⁹R. Marriott and M. Rotenberg, *Phys. Rev. Letters* 21, 722 (1968).

²⁰K. Omidvar, *Phys. Rev.* 133, A970 (1964).

²¹J. Wm. McGowan, E. M. Clarke, and E. K. Curley, *Phys. Rev. Letters* 15, 917 (1965); 17E, 66 (1966).

²²H. Kleinpoppen and E. Kraiss, *Phys. Rev. Letters* 20, 361 (1968).